Excited-State Cis–Trans Isomerization of *cis*-Hexatriene. A CAS-SCF Computational Study

Massimo Olivucci,*,† Fernando Bernardi,† Paolo Celani,† Ioannis Ragazos,‡ and Michael A. Robb*,‡

Contribution from the Dipartimento di Chimica "G.Ciamician" dell'Universita di Bologna, Via Selmi 2, 40126 Bologna, Italy, and Department of Chemistry, King's College, London, Strand, London WC2R 2LS, U.K.

Received January 28, 1993. Revised Manuscript Received October 25, 1993®

Abstract: Two different reaction pathways for the cis–trans isomerization of *cis*-hexa-1,3,5-triene in its first excited (2^1A_g) state have been determined using the CAS-SCF (six-orbital/six-electron active space) and CAS-SCF/MP2 methods with 4-31G and DZ+d basis sets. Intrinsic reaction coordinate calculations demonstrate that these pathways correspond to c/t and Z/E interconversion of the initial *cis*-hexatriene (*tZt*) isomer. However, these two isomerization processes do not terminate on the excited-state potential energy surface since both the c/t and Z/E pathways lead to "products" which are located at only one-third of the way along the "expected" (i.e., 180° rotation) reaction coordinates. The two excited-state "product" wells, which are both entered by overcoming small barriers (4 and 6 kcal mol^{-1}), correspond to two different Born–Oppenheimer violation regions centered on two low-lying conical intersection points. Thus, while an excited-state *cis*-hexatriene molecule can easily initiate a cis–trans isomerization process, this process can be completed only on the ground-state potential energy surface after passage through a conical intersection where a fast, radiationless decay is possible. The existence of these nonadiabatic reaction pathways is consistent with the available experimental data on the photochemistry and photophysics of *cis*-hexatrienes.

1. Introduction

Direct irradiation of hexa-1,3,5-trienes yields a rather complex mixture of photoproducts[1] which includes cis–trans isomers, cyclohexa-1,3-dienes, bicyclo[3.1.0]hex-2-enes, and vinylcyclobutenes. In these photoreactions, rotation about one or more double bonds leads to partial or complete cis–trans isomerization. Like other photochemical events, these isomerizations are nonadiabatic processes and thus occur along a two-part pathway which starts on the excited state and continues, after passing through a Born–Oppenheimer violation region, on the ground state.

In several organic reactivity problems,[2] we have characterized this Born–Oppenheimer violation region and shown that it is associated with a conical intersection of the excited- and ground-state potential energy surfaces. At a conical intersection, a fast, radiationless decay to the ground state is possible,[3] and the structure and energetic accessibility of the conical intersection can determine the type and yield of the possible photoproducts. In other words, since in the region surrounding a conical intersection point there is a large probability of decay, the excited-state system enters a ground-state pathway only after this region of the excited-state surface has been accessed. Thus the conical intersection structure acquires, in a photochemical process, the same meaning that a transition state has for a thermal reaction and is the central mechanistic feature of this type of nonadiabatic process. These mechanistic features have been recently elucidated in a CAS-SCF/4-31G study of the 2^1A_g potential energy surface of buta-1,3-diene,[4] where we have demonstrated that accessible conical intersection points exist along distinct cis–trans isomerization pathways which originate in either the s-cis or the s-trans excited-state butadiene wells. These conical intersections provide efficient radiationless decay channels that are easily accessible by overcoming a small (<2 kcal/mol) barrier or via a barrierless pathway from the s-cis or the s-trans well, respectively. Recent spectroscopic observations[5] suggest that low-frequency modes dominated by cis–trans motion are indeed involved in the opening of radiationless decay channels on the first excited (2^1A_g) state of short polyenes. Most importantly, Christensen, Yoshihara, Bell, and Petek[5a] have recently demonstrated that the fluorescence excitation spectra of *cis*-hexa-1,3,5-triene (or, more simply, *cis*-hexatriene) and octa-2,4,6-triene are consistent with the existence of at least two different very fast, radiationless decay channels in *cis*-hexatrienes with a barrier below 1 kcal/mol. They suggest that at least one of these radiationless decay channels is accessible via cis–trans isomerization motion.

Our previous work on a conical intersection mechanism for the photochemistry of butadiene[4] and the recent experimental work of Christensen, Yoshihara, Bell, and Petek[5a] provide the motivation for the present article, in which we report a numerical investigation (CAS-SCF/4-31G and DZ+d) of the cis–trans isomerization pathways on the first excited (2^1A_g)[5c] potential energy surface of *cis*-hexatriene (although in C_{2v} *cis*-hexatriene the correct symmetry label is A_1 instead of A_g, we use the C_{2h} label to emphasize the connection to the corresponding state of *trans*-hexatriene). We have studied not only the region surrounding the excited-state minimum but also a much larger region mainly spanned by torsions about the double and single bonds of the

† Universita di Bologna.

‡ King's College.

® Abstract published in *Advance ACS Abstracts,* December 1, 1993.

(1) (a) Jacobs, H. J. C.; Havinga, E. Photochemistry of Vitamin D and Its Isomers and of Simple Trienes. In *Advances in Photochemistry*; Pitts, J. N., Jr., Hammond, G. S., Gollnick, K., Eds.; John Wiley & Sons: New York, 1979; Vol. 11, pp 305–373. (b) Dauben, W. G.; McInnis, E. L.; Mincho, D. M. Photochemical rearrangements in trienes. In *Rearrangements in ground and excited states*; De Mayo, P., Ed.; Academic Press: London, 1980; Vol. 3, pp 91–129. (c) Vroegop, P. J.; Lugtenburg, J.; Havinga, E. *Tetrahedron* **1973**, *29*, 1393–1398. (d) Dauben, W. G.; Rabinowitz, J.; Vietmeyer, N. D.; Wendscuh, P. H. *J. Am. Chem. Soc.* **1972**, *94*, 4285–4292.

(2) (a) Bernardi, F.; De, S.; Olivucci, M.; Robb, M. A. *J. Am. Chem. Soc.* **1990**, *112*, 1737–1744. (b) Bernardi, F.; Olivucci, M.; Robb, M. A. *Acc. Chem. Res.* **1990**, *23*, 405–412. (c) Bernardi, F.; Olivucci, M.; Ragazos, I. N.; Robb, M. A. *J. Am. Chem. Soc.* **1992**, *114*, 2752–2754. (d) Bernardi, F.; Olivucci, M.; Robb, M. A.; Tonachini, G. *J. Am. Chem. Soc.* **1992**, *114*, 5805–5812. (e) Bernardi, F.; Olivucci, M.; Ragazos, I. N.; Robb, M. A. *J. Am. Chem. Soc.* **1992**, *114*, 8211–8220.

(3) Manthe, U.; Koppel, H. *J. Chem. Phys.* **1990**, *93*, 1658–1669.

(4) Olivucci, M.; Bernardi, F.; Ragazos, I. N.; Robb, M. A. *J. Am. Chem. Soc.* **1993**, *115*, 3710–3721.

(5) (a) Petek, H.; Bell, A. J.; Christensen, R. L.; Yoshihara, K. *J. Chem. Phys.* **1992**, *96*, 2412–2415. (b) Ci, X.; Myers, A. B. *J. Chem. Phys.* **1992**, *96*, 6433–6441. (c) Buma, W. J.; Kohler, B. E.; Song, K. *J. Chem. Phys.* **1991**, *94*, 6367–6375.

0002-7863/94/1516-1077$04.50/0

carbon framework. As we will subsequently discuss, our findings are consistent with a novel mechanistic picture of hexatriene photochemistry which is based upon the existence of two distinct conical intersections between the excited- and ground-state potential energy surfaces. Surprisingly, the two conical intersections are accessible via two different transition states located at about one-third (60.0° rotation) of the way along two distinct cis–trans isomerization pathways. Thus, while excited-state *cis*-hexatriene can easily initiate a cis–trans isomerization process on the excited state, this process can be completed only on the ground-state potential energy surface after passage through a conical intersection region. As mentioned above, these regions of the excited-state surface provide efficient channels for the radiationless decay of an excited-state molecule, thus contributing to decrease its fluorescence quantum yield. Although the magnitude of the computed barriers to the two-conical-intersection region in *cis*-hexatriene is different from those reported by Christensen, Yoshihara, Bell, and Petek,[5a] we believe that the existence of those features on the excited-state potential energy surface could indeed play a role in explaining their experimental observation and, in general, the very low fluorescence quantum yield in hexatrienes.

2. Theoretical and Computational Methods

All the CAS-SCF results presented in this paper have been produced using the MC-SCF program distributed in Gaussian 92.[6] Location of excited-state minima and transition structures and calculations of intrinsic reaction coordinates (IRC) have been carried out by using the methods available in the same program package. However, the location of the "funnels" corresponding to low-lying conical intersection points requires a nonstandard method,[7] which we will now briefly summarize. This nonstandard method has been implemented in a development version of the Gaussian package.

A conical intersection of two potential energy surfaces is defined by the following statement:[8] *Two states, even with the same symmetry, may intersect along an* $(n-2)$*-dimensional hyperline as the energy is plotted against the n nuclear coordinates.*

While such topological features have been extensively discussed in the literature,[9] quantitative "ab initio" data on conical intersections of potential energy surfaces are, especially for organic systems, quite limited. This is probably due to the fact that these features have been considered rather unusual. However, recent CAS-SCF investigations have indicated that the conical intersections can be a common feature in organic[2] and inorganic systems.[10] We have recently implemented, at the CAS-SCF level, a new method for the optimization of the lowest energy point on a conical intersection of two potential energy surfaces,[7] which we now describe.

The nature of the potential energy surfaces near a conical intersection point has been recently described by Ruedenberg *et al.*,[11] and it is convenient to use their terminology. In Scheme 1, we show a conical intersection of two potential energy surfaces as a "curve" spanning an $(n-2)$-dimensional subspace of the n nuclear coordinates called *intersection space*.

Scheme 1

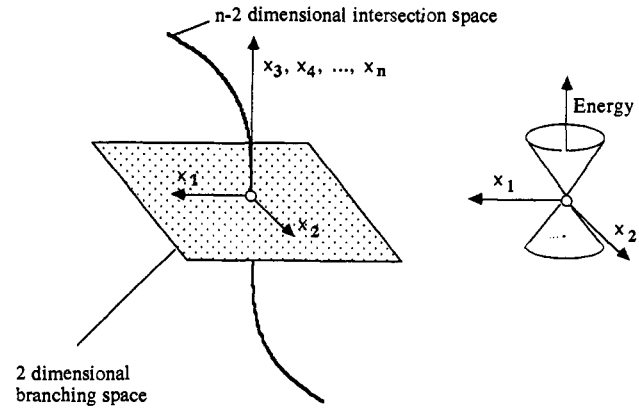

While for any point belonging to the intersection space (i.e., any point of the curve in Scheme 1) the energies of the two states remain the same, the degeneracy is lifted when the geometry of the system is distorted along the two remaining linearly independent nuclear coordinates $\mathbf{x}_1$ and $\mathbf{x}_2$. Thus, when the energy of the two states is plotted in the *branching space* (i.e., against $\mathbf{x}_1$ and $\mathbf{x}_2$), as shown in Scheme 1, the corresponding potential energy surfaces look like a double cone. The optimized conical intersection structure corresponds to the lowest energy point in the $(n-2)$-dimensional intersection space. Such a point is defined by two conditions: (i) the energies of the two states must be equal and (ii) the projection of the energy gradient (of either state) onto the intersection space is zero. The method we use is based on a Lagrangian multiplier technique and is documented in ref 7. Note that the gradient on the excited-state potential energy surface will not be zero because the excited- (and ground-) state potential energy surface "looks like" the vertex of a cone along the branching space.

The two vectors $\mathbf{x}_1$ and $\mathbf{x}_2$ have a dynamic significance which can be discussed qualitatively in the framework of simple semiclassical methods like the trajectory surface hopping (TSH) treatment.[12] The photoexcited system will move, during its excited-state lifetime, along classical trajectories that in the limit of the very low temperatures can be represented by the intrinsic reaction coordinates located on the excited-state sheet. When such a pathway terminates in the vicinity of a conical intersection point (i.e., in the Born–Oppenheimer violation region surrounding it), the system undergoes a "surface hop", i.e., a radiationless decay from the excited state to the ground state. After the hop, the direction of the original excited-state motion, i.e., the momentum on the excited state, will not, in general, be conserved. When the transition occurs, in order to conserve total energy, one must adjust a component of the momentum in the direction of the $\mathbf{x}_2$ or $\mathbf{x}_1$ vector[12c] or, in other words, on the plane orthogonal to the intersection space which corresponds, locally, to the branching space. Thus when the hop occurs in the vicinity of a conical intersection point, the direction of the motion after the decay from the excited to the ground state will be diverted along one of the directions contained in the plane formed by the vectors $\mathbf{x}_1$ and $\mathbf{x}_2$. Finally, one should point out that at the minimum energy point on the conical intersection, the gradients of both ground and excited states will be zero in all directions except $\mathbf{x}_1$ or $\mathbf{x}_2$. Thus, if the system had no initial momentum at the conical intersection, the initial decay paths would lie in the branching space. Thus, the main initial decay paths from the conical intersection will lie in the plane $\mathbf{x}_1\mathbf{x}_2$ (i.e., in the branching space) unless the conical intersection is entered with significant momentum along a path orthogonal to these directions.

(6) Frisch, M. J.; Trucks, G. W.; Head-Gordon, M.; Gill, P. M. W.; Wong, M. W.; Foresman, J. B.; Johnson, B. G.; Schlegel, H. B.; Robb, M. A.; Replogle, E. S.; Gomperts, R.; Andres, J. L.; Raghavachari, K.; Binkley, J. S.; Gonzalez, C.; Martin, R. L.; Fox, D. J.; Defrees, D. J.; Baker, J.; Stewa rt, J. J. P.; Pople, J. A. *Gaussian 92*, Revision B; Gaussian, Inc.: Pittsburgh, PA, 1992.

(7) Ragazos, I. N.; Robb, M. A.; Bernardi, F.; Olivucci, M. *Chem. Phys. Lett.* **1992**, *197*, 217–223.

(8) Salem, L. *Electrons in Chemical Reactions: First Principles*; Wiley: New York, 1982.

(9) (a) Von Neunann, J.; Wigner, E. *Physik. Z.* **1929**, *30*, 467. (b) Teller, E. *J. Phys. Chem.* **1937**, *41*, 109. (c) Herzberg, G.; Longuet-Higgins, H. C. *Trans. Faraday Soc.* **1963**, *35*, 77. (d) Herzberg, G. *The Electronic Spectra of Polyatomic Molecules*; Van Nostrand: Princeton, 1966; p 442. (e) Mead, C. A.; Truhlar, D. G. *J. Chem. Phys.* **1979**, *70*, 2284. (f) Mead, C. A. *Chem. Phys.* **1980**, *49*, 23. (g) Keating, S. P.; Mead, C. A. *J. Chem. Phys.* **1985**, *82*, 5102. (h) Keating, S. P.; Mead, C. A. *J. Chem. Phys.* **1987**, *86*, 2152. (i) Gerhartz, W.; Poshusta, R. D.; Michl, J. *J. Am. Chem. Soc.* **1977**, *99*, 4263. (j) Michl, J.; Bonacic-Koutecky, V. *Electronic Aspects of Organic Photochemistry*; Wiley: New York, 1990. (k) Bonacic-Koutecky, V.; Koutecky, J.; Michl, J. *Angew. Chem., Int. Ed. Engl.* **1987**, *26*, 170–189. (l) Davidson, R. E.; Borden, W. T.; Smith, J. *J. Am. Chem. Soc.* **1978**, *100*, 3299–3302. (m) Mead, C. A. The Born–Oppenheimer approximation in molecular quantum mechanics. In *Mathematical frontiers in computational chemical physics*; Truhlar, D. G., Ed.; Springer: New York, 1987; Chapter 1, pp 1–17. (n) Tully, J. C.; Preston, R. K. *J. Chem. Phys.* **1971**, *55*, 562. Dehareng, D.; Chapuisat, X.; Lorquet, J. C.; Galloy, C.; Raseev, G. *J. Chem. Phys.* **1983**, *78*, 1246–1264. Blais, N. C.; Truhlar, D. G.; Mead, C. A. *J. Chem. Phys.* **1988**, *89*, 6204–6208.

(10) (a) Atchity, G. J.; Xantheas, S. S.; Elbert, S. T.; Ruedenberg, K. *J. Chem. Phys.* **1991**, *94*, 8054–8069. (b) Atchity, G. J.; Xantheas, S. S.; Elbert, S. T.; Ruedenberg, K. *Theor. Chim. Acta* **1991**, *78*, 365. (c) Muller, H.; Koppel, H.; Cederbaum, L. S.; Schmelz, T.; Chambaud, G.; Rosmus, P. *Chem. Phys. Lett.* **1992**, *197*, 599–606. (d) Manaa, M. R.; Yarkony, D. R. *J. Chem. Phys.* **1990**, *93*, 4473. (e) Manaa, M. R.; Yarkony, D. R. *J. Chem. Phys.* **1992**, *97*, 715–717.

(11) Atchity, G. J.; Xantheas, S. S.; Ruedenberg, K. *J. Chem. Phys.* **1991**, *95*, 1862–1876.

(12) (a) Tully, J. C.; Preston, R. K. *J. Chem. Phys.* **1971**, *55*, 562. (b) Dehareng, D.; Chapuisat, X.; Lorquet, J. C.; Galloy, C.; Raseev, G. *J. Chem. Phys.* **1983**, *78*, 1246–1264. (c) Blais, N. C.; Truhlar, D. G.; Mead, C. A. *J. Chem. Phys.* **1988**, *89*, 6204–6208.

Scheme 2

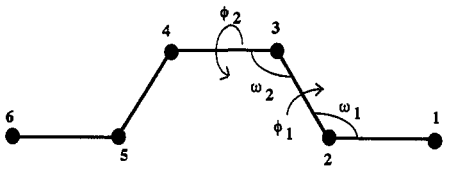

tZt -hexatriene

To conclude this section, some comments on the relability of the methods used are in order. The choice of active space in our CAS-SCF computations is unambiguous and is comprised of the six electrons and orbitals which form the π-system of hexatriene. The 175-term CAS-SCF wave function is capable of describing all the states that can arise from all possible arrangements of six electrons in six orbitals. *All the orbitals are fully utilized and optimized* in the computation, but only the active orbitals can have variable occupancy. Thus no assumption of σ/π separability is implied. The identification of six p^π active orbitals is merely a specification of which orbitals can have occupancy other than 2. As the geometry is changed from a planar arrangement, the optimization of the orbitals mixes σ/π orbitals to give the lowest energy. (The only type of interaction that is not included explicitly at the CI level would result from single excitations of the σ backbone. However, this type of interaction is included through the Brillouin condition satisfied by the optimum MC-SCF orbitals). Thus, the mixing of singly excited states that can occur for nonplanar geometries is treated without any approximation.

Now we turn to the limitations on our calculations that arise from the basis set used. Since we have explored the excited-state surfaces and the Born–Oppenheimer violation region in considerable detail, we have restricted ourselves to modest 4-31G and DZ+d basis sets. This is adequate to determine the surface topology and optimized geometries of the covalent states. However, in order to obtain a description of the ionic states (singly excited states or Rydberg states), a basis set containing diffuse functions and an increased active space consisting of both "tight" and "diffuse" p^π orbitals are required.[13] Roos *et al.*[13b-d] have run very accurate benchmark computations on the excited states of benzene, *s-trans*-butadiene, and *tEt*-hexatriene. They show that while the description of the ionic and Rydberg states is sensitive to basis sets, the number of active orbitals, and electron correlation, the covalent states are well described by a 6-active-orbital space. The quality of the DZ+d basis set used in our computations has been tested against the ANO basis set used by Roos for the computation of the excitation energies of the *s-trans*-butadiene and *tEt*-hexatriene 2^1A_g states. Using ground-state CAS-SCF/DZ+d optimized geometries for these two systems, we have been able to reproduce the published CAS-SCF/ANO data[13d] within the reported computational error. Our calculations therefore offer a reliable description of the lowest energy singlet covalent states which are of central importance[5] in the photochemical and photophysical processes. However, since our results show that the optimum structures of the *tZt*-hexatriene low-lying conical intersection points are rather far away from the correspondent excited-state minimum, we have also investigated the effects of d-type polarization functions, sp-type diffuse functions, and dynamic correlation energy on the nature and energy of the covalent states. In particular, the existence of the conical intersection points found has been confirmed via single-point CAS-SCF/MP2 computation using the DZ+d basis set. The CAS-SCF/MP2 method has been documented and tested elsewhere[14] and provides a convenient alternative to other more expensive methods (for instance, MR-CI) for the evaluation of the electronic energy in the presence of dynamic correlation. As we will document below, the results of these calculations show no change in the nature of the excited state in these regions.

3. Characterization of the 2^1A_g Potential Energy Surface of *cis*-Hexatriene

To our knowledge, the only previous ab initio CAS-SCF calculations on the 2^1A_g state of *cis*-hexatriene are those of Buma, Kohler, and Song.[5c] Buma *et al.* have optimized the geometry of the *tZt*-hexatriene minimum using a DZ basis set. The optimized *tZt*-hexatriene structure was found to correspond to a planar C_{2v} molecule. The result of this ab initio calculation is partly in agreement with the vibrational analysis of the $1^1A_g \rightarrow 2^1A_g$ REMPI excitation spectrum, which shows that the 2^1A_g *cis*-hexatriene structure has two different conformers. Buma *et al.*[5c] demonstrated that the two terminal CH_2 groups are extremely floppy since the energy increases only 5 cm^{-1} when these two groups are distorted from the molecular plane via out-of-plane bending.

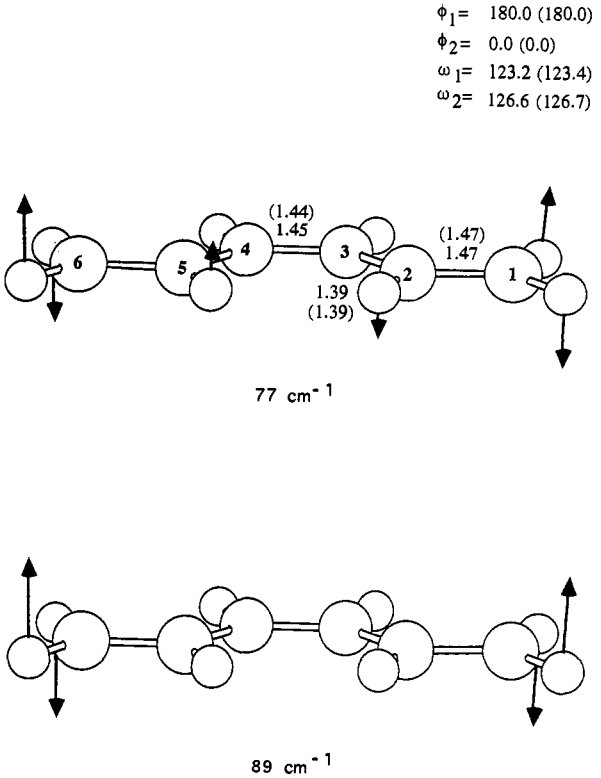

Figure 1. CAS-SCF excited-state *tZt*-hexatriene equilibrium structure. The main structural parameters are reported (bond lengths in angstroms and bond angles in degrees) for both the 4-31G and the DZ+d (in parentheses) results. Parameters ϕ_1, ϕ_2, ω_1, and ω_2 are defined in Scheme 2. The arrows indicate the directions of the nuclear displacements corresponding to the two CAS-SCF/4-31G lowest frequency normal modes.

As a starting point for our investigation of the 2^1A_g state of *cis*-hexatriene, we repeated the CAS-SCF search and optimization of the *tZt*-hexatriene isomer using both the standard 4-31G and Dunning DZ+d basis set (diffuse (d) functions have been added on heavy atoms) with an active space of six active electrons and six active orbitals corresponding to the six p^π orbitals of planar hexatriene. These calculations yielded an optimized C_{2v} structure in agreement with the results reported above. However, the result of a frequency calculation at the 4-31G level shows that the floppiest vibrational motions in this molecule correspond to torsions of the two terminal methylenes rather than to out-of-plane bendings as suggested in ref 5c. In Figure 1, we give the values of the relevant geometrical parameters (torsional and bending geometrical parameters are defined in Scheme 2 above) for the fully optimized structure together with a pictorial representation of the motion associated with the two floppiest (77 and 89 cm^{-1}) normal modes of the molecule. The first mode leads to distortion of the planar C_{2v} structure toward a nonplanar C_2 structure, while the second mode leads to a nonplanar C_s structure. In both of these normal modes there are small carbon framework contributions coupled to the CH_2 torsional motion.

Our main objective in this work is to document the 2^1A_g potential energy surface in a region far from the excited-state

(13) (a) Serrano-Andrés, L.; Merchan, M.; Nebot-Gil, I.; Lindh, R.; Roos, B. O. *J. Chem. Phys.* **1993**, *98*, 3151–3162. (b) Matos, J. M. O.; Roos, B. O.; Malmqvist, P.-Å. *Chem. Phys.* **1987**, *86*, 1458–1466. (c) Roos, B. O.; Andersson, K.; Fülscher, M. P. *Chem. Phys. Lett.* **1992**, *192*, 5–13. (d) Serrano-Andrés, L.; Merchan, M.; Nebot-Gil, I.; Lindh, R.; Roos, B. O. *J. Chem. Phys.* **1993**, *98*, 3151–3162.

(14) Bernardi, F.; Bottoni, A.; Celani, P.; Olivucci, M.; Robb, M. A. Venturini, A. *Chem. Phys. Lett.* **1992**, *192*, 229–235.

Scheme 3

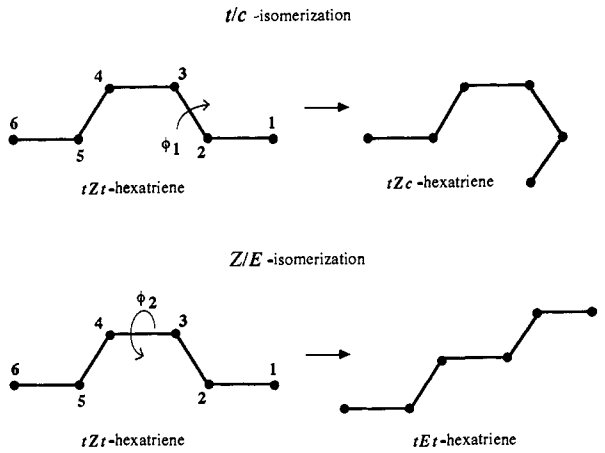

minimum. In particular, we wish to locate the possible hexatriene cis–trans isomerization pathways on this surface. In Scheme 3 we show the two main isomerization processes in *tZt*-hexatriene. Coordinate ϕ_1 (see Scheme 3 above) would be expected to dominate a cis–trans (c/t) isomerization pathway connecting the different conformers (*tZt* and *tZc*) of hexatriene. The second torsional coordinate, ϕ_2 (see Scheme 3 above), describes a *real* ground-state cis–trans (Z/E) isomerization, where a Z isomer is transformed into the corresponding E isomer (*tZt* to *tEt*) without altering the geometrical arrangement about the two single bonds (bonds 2–3 and 4–5 in Scheme 2). Thus, while we will use, in the following, the generic term "cis–trans isomerization" for indicating both of the two types of isomerizations described above, we will refer to a specific pathway using the label c/t or Z/E.

The search for critical points along pathways dominated by either ϕ_1 or ϕ_2 has been carried out using both the 4-31G and the DZ+d basis sets. We find two distinct transition structures that we indicate by $TS_{c/t}$ and $TS_{Z/E}$ in Figures 2a and 2b, respectively, where the structural parameters are given along with the two corresponding transition vectors (determined by analytical frequency calculation at the 4-31G basis set level). The actual values of the two torsional coordinates ϕ_1 and ϕ_2 are surprising. The torsional coordinate ϕ_1 might be expected to have a value near 90° in a transition structure for c/t isomerization. However, we find a value near 120° for ϕ_1 in $TS_{c/t}$, which indicates that the transition structure is located at one-third of the way along the isomerization path. Furthermore, the transition vector of $TS_{c/t}$ involves additional geometrical parameters. In particular, there is a significant contribution from ϕ_2 and from the bending angle ω_1. Notice that the carbon framework of the system is considerably distorted in addition to the expected change in ϕ_1. In particular, the ethylene group is twisted (the terminal CH_2 group on carbon 1 is rotated about 45°). Similarly, for $TS_{Z/E}$ one observes that the value of the torsional parameter ϕ_2 is 60° (instead of the ideal 90°) and that ϕ_1, bending angle ω_2, and the torsional angle of the terminal CH_2 group all contribute significantly to the transition vector. Remarkably, the values of ϕ_1 and of the CH_2 torsion are large and almost of the same magnitude of ϕ_2 itself. Thus, both of the transition structures occur at about one-third of the way along the two idealized cis–trans isomerization pathways.

While the only possible reactant excited-state well accessible from the two transition structures is that corresponding to the *tZt* minimum previously described, the nature of the excited-state products is not obvious from the structure of the two transition states. In fact, the excited-state product wells that would be expected to lie on a reaction path from these two transition states do not actually correspond to any true excited-state equilibrium structures but to two distinct singularities (two conical intersections) where the excited state and the ground state are

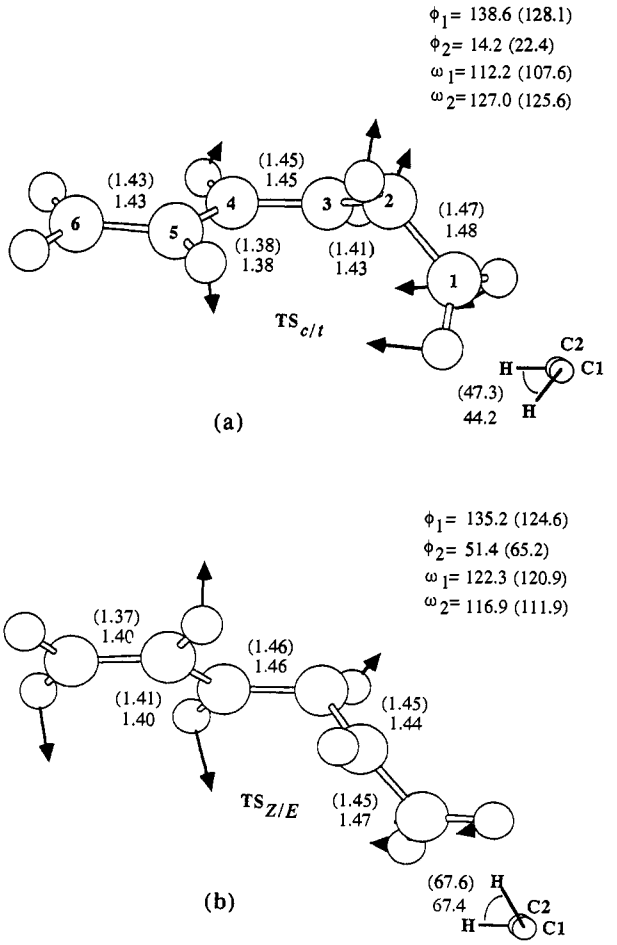

Figure 2. Optimized CAS-SCF excited state c/t (a) and Z/E (b) transition structures. The main structural parameters are reported (bond lengths in angstroms and bond angles in degrees) for both the 4-31G and the DZ+d (in parentheses) results. Parameters ϕ_1, ϕ_2, ω_1, and ω_2 are defined in Scheme 2. The arrows indicate the direction of the nuclear displacements corresponding to the CAS-SCF/4-31G transition vectors.

degenerate. In order to document this feature and gain further insight into the nature of the excited-state isomerization pathways, we have computed the intrinsic reaction coordinates (IRC) starting from the two excited-state transition structures. The evolution of the reactant hexatriene structure along the IRC is shown in Figures 3 and 4 for the t/c and Z/E isomerization paths, respectively. The two corresponding energy profiles which are shown in Figure 5 are reported as functions of the dominant torsional coordinate. The values of the other important geometrical parameters are also reported in the figure. The initial distortion of the reactant geometry associated with the c/t isomerization pathway (Figure 5a) is likely to originate from a motion similar to that described by its lowest frequency normal mode (see Figure 1), which then mixes with other modes to generate the asymmetric structure **I** in Figure 3. The evolution of this structure toward the transition state is mainly characterized by the decreasing of the torsional angle ϕ_1 and the bending angle ω_1. The contribution of this last geometrical parameter increases after point **III** as the system moves closer to the transition structure and becomes almost dominant beyond it. The evolution of the reactant structure along the Z/E isomerization pathway (Figure 5b) is described by the change in the value of the torsional angle ϕ_2 and the bending angle ω_2, although the torsional coordinate associated with the terminal CH_2 group and with ϕ_1 seems to be strongly coupled to ϕ_2. The bending angle ω_2 increases in importance as one approaches $TS_{Z/E}$ in a similar fashion to the behavior shown by ω_1 along the c/t path and, again, almost dominates beyond the TS.

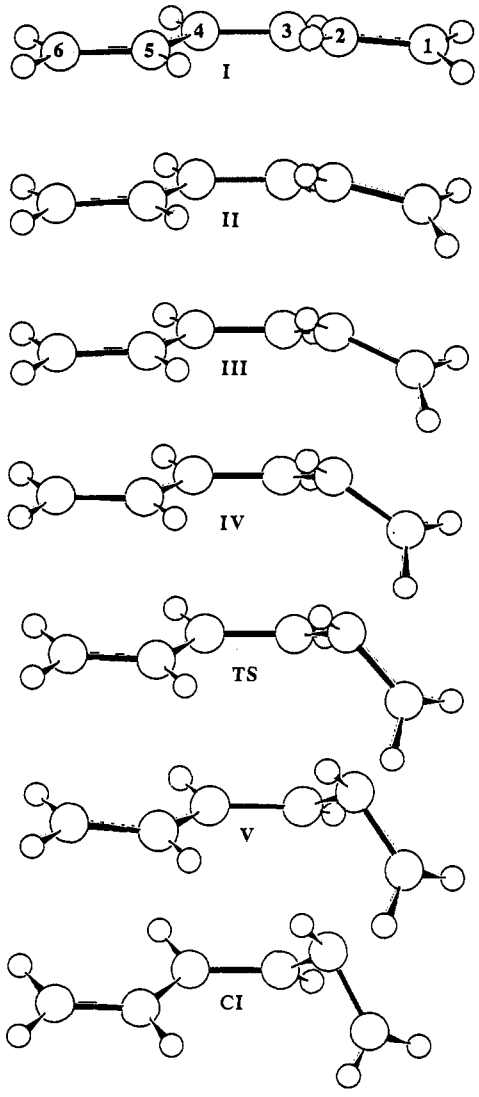

Figure 3. Evolution of the *tZt*-hexatriene equilibrium structure along the *c*/*t* IRC computed at the CAS-SCF/4-31G level. TS indicates the *c*/*t* transition structure (see Figure 2a) and CI the corresponding optimized conical intersection structure.

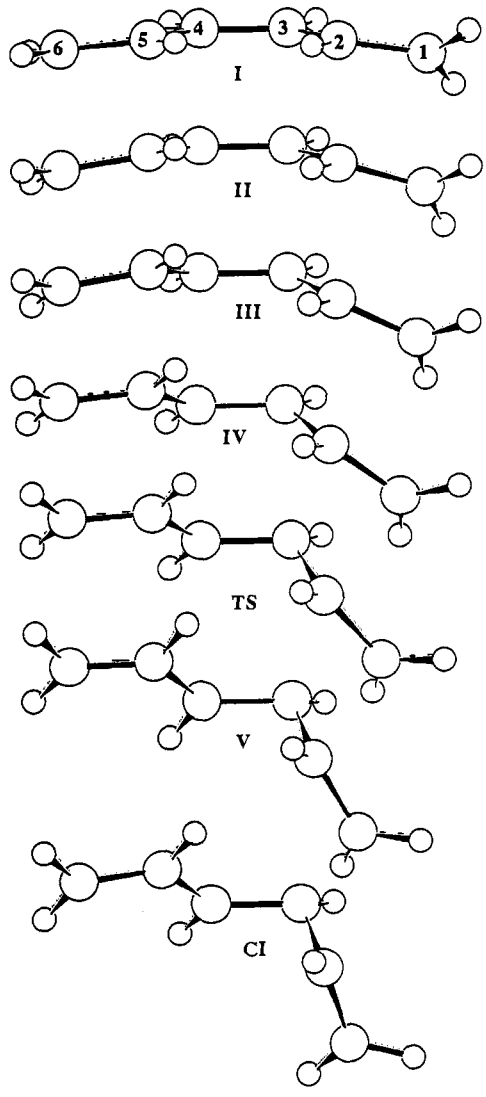

Figure 4. Evolution of the *tZt*-hexatriene equilibrium structure along the *Z*/*E* IRC computed at the CAS-SCF/4-31G level. TS indicates the *Z*/*E* transition structure (see Figure 2b) and CI the corresponding optimized conical intersection structure.

Table 1. Absolute (*E*) and Relative (ΔE) CAS-SCF and CAS-SCF/MP2 (values in parentheses) Energies for the Stationary Points and Conical Intersections of S_1 *tZt*-Hexatriene

structure	root	*E*/4-31G, a.u.	*E*/DZ+d, a.u.	ΔE/4-31G, kcal mol^{-1}	ΔE/DZ+d, kcal mol^{-1}
reactant	S_1	−231.401 74	−231.754 61	0.0	0.0
$TS_{c/t}$	S_1	−231.392 26	−231.748 52	5.95	3.82
$TS_{Z/E}$	S_1	−231.387 96	−231.744 85	8.65	6.12
$CI_{c/t}$	S_1[a]	−231.390 11	−231.745 65[c]		
			(−232.453 27)[c]		
	S_0[a]	−231.390 81	−231.749 18[c]		
			(−232.457 53)[c]		
	S_1[a,b]	−231.400 88	−231.747 73[c]		
	S_0[a,b]	−231.401 54	−231.751 22[c]		
$CI_{Z/E}$	S_1[a]	−231.382 46	−231.740 80[c]		
			(−232.441 77)[c]		
	S_0[a]	−231.382 50	−231.736 05[c]		
			(−232.447 82)[c]		
	S_1[a,b]	−231.392 75	−231.738 03[c]		
	S_0[a,b]	−231.393 20	−231.742 78[c]		

[a] Indicates state-averaged CAS-SCF calculation. See ref 7. [b] Basis set augmented with sp-type diffuse functions. See ref 18. [c] Energy value computed at the CAS-SCF/4-31G optimized structure.

The behavior of the ground-state energy along the IRC is indicated in Figure 6. One observes a continuous decrease in energy difference between the ground and excited states along the IRC, and both the IRCs terminate, after the transition structure, in a point where one has a degeneracy between the first and the second root of the secular problem. In these regions, the ground- and excited-state potential energy surfaces merge in two distinct conical intersections. The geometries of the two local minima on the conical intersections $CI_{c/t}$ and $CI_{Z/E}$ have been optimized using the method outlined in the previous section, and the geometrical parameters are shown in Figure 7b and 8b. The stability of the degeneracy between the first and second roots at $CI_{c/t}$ and $CI_{Z/E}$ has been tested by improving the 4-31G basis set with sp-type diffuse functions.[19] As anticipated in section 2, the data in Table 1 show that the degeneracy is not sensitive to the presence of diffuse functions in the basis set. The same test has been performed by improving the basis set (i.e., using the DZ+d and DZ+spd basis sets) and by performing CAS-SCF/MP2 computations (see section 2) with the DZ+d basis set. The results in Table 1 demonstrate that neither the improvement of the basis set nor the evaluation of dynamic correlation energy via CAS-SCF/MP2 removes the degeneracy (small S_1/S_0 gaps in Table 1 around 3 kcal mol^{-1} arise because the energies are evaluated via single-point computations on the $CI_{c/t}$ and $CI_{Z/E}$ optimized at the CAS-SCF/4-31G level). It is easy to recognize from the molecular structures that the two conical intersection minima correspond to the final points of the two excited-state reaction pathways (i.e., they are the next structure along the IRC after

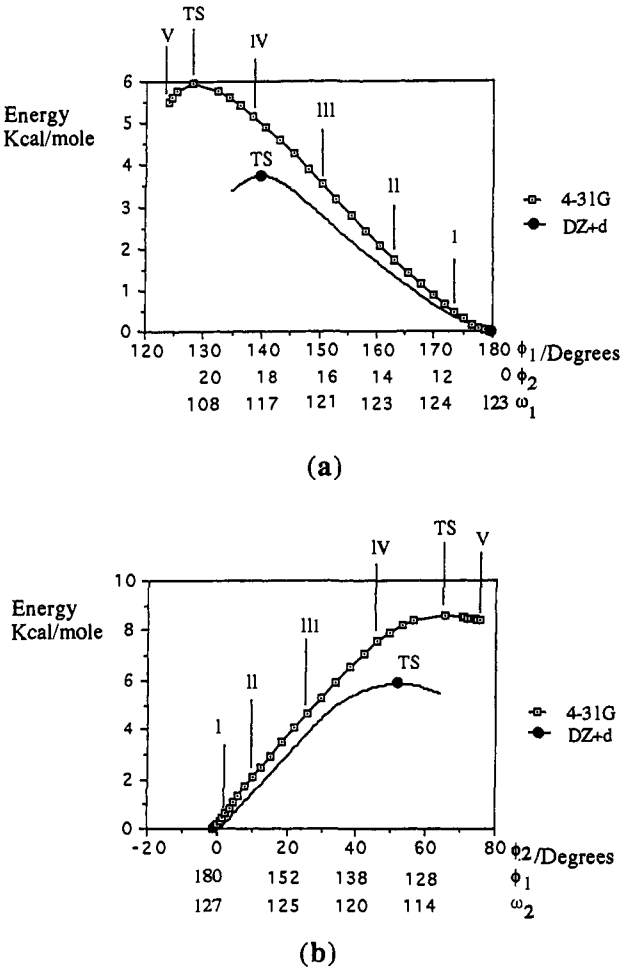

Figure 5. Excited-state energy profiles along the c/t (a) and Z/E (b) IRCs computed at the CAS-SCF/4-31G level and plotted against the relevant geometrical parameters (ϕ_1, ϕ_2, ω_1, and ω_2 are defined in Scheme 2). The position (relative to the reactant) of a few IRC structures (see Figures 3 and 4 for the labels) and of the DZ+d transition structures have also been reported in the figure.

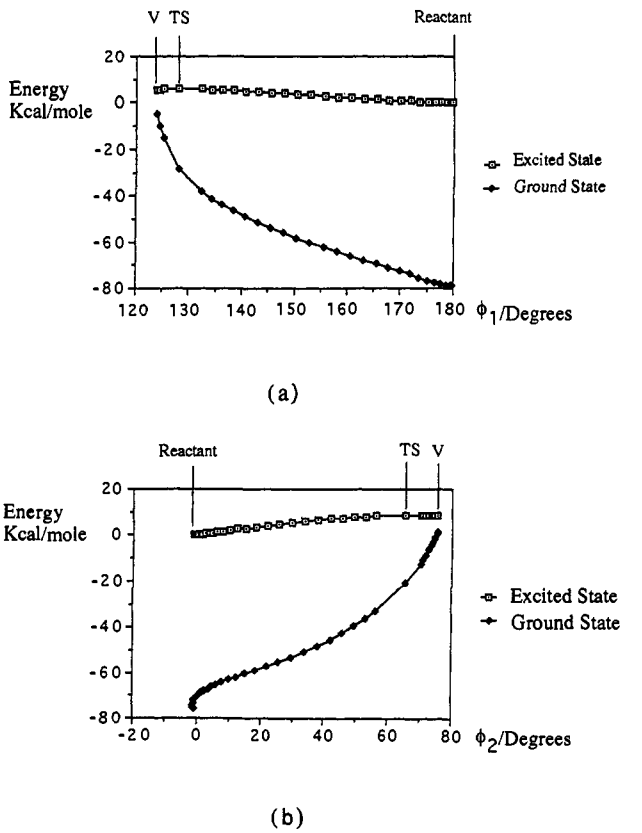

Figure 6. Excited- and ground-state energy profiles along the c/t (a) and Z/E (b) IRCs computed at the CAS-SCF/4-31G level and plotted against the torsional angles ϕ_1 and ϕ_2, respectively (ϕ_1 and ϕ_2 are defined in Scheme 2).

point V, as shown in Figures 3 and 4). However, they are far from the cis–trans isomerization products. In fact, while $CI_{c/t}$ and $CI_{Z/E}$ are final points of two *excited-state* pathways, they can be seen as starting points of two related ground-state pathways which begin at the conical intersection region and lead ultimately to the final *ground-state* products. We will discuss this mechanistic view of photoisomerizations in the next section.

The efficiency of the decay path from the two isomerization pathways discussed above depends on the accessibility of the two conical intersections from the excited-state *tZt*-hexatriene well (i.e., the magnitude of the barriers on the path to the two transition structures $TS_{c/t}$ and $TS_{Z/E}$). The energetics are summarized in Table 1. While the magnitude of the two barriers (about 6 and 4 kcal mol^{-1}) is larger than the experimental values,[5a] the barriers are very small and sensitive to the basis set used in the calculation. In addition, the geometries of the transition states $TS_{c/t}$ and $TS_{Z/E}$ shift toward the *cis*-hexatriene minimum as the basis set (see Figure 5) is improved. However, the main topological features of the potential energy surface (the existence of transition structures on a cis–trans isomerization reaction path leading to conical intersections) are independent of the basis set used.

A final point of interest concerns the relationship between the IRC direction and the branching space spanned (locally) by the vectors $\mathbf{x}_1$ and $\mathbf{x}_2$ in Scheme 1. When the surface hop occurs in the vicinity of a conical intersection point and the system is moving along the IRC, the direction of the motion after the decay from the excited to the ground state will be partly diverted from the IRC direction along one of the directions contained in the plane formed by the vectors $\mathbf{x}_1$ and $\mathbf{x}_2$. As we have discussed elsewhere[4] and briefly illustrated in the previous section, this branching space (associated with a conical intersection point like $CI_{c/t}$ or $CI_{Z/E}$) is spanned by the nonadiabatic coupling (NADC) and the gradient difference (GD) vectors which are computed during the optimization process. In Figures 7 and 8, we have reported a schematic representation of the main components of the vectors GD and NADC for the conical intersection $CI_{c/t}$ and $CI_{Z/E}$, respectively. In the same figures we also give the IRC vector corresponding to structure V for either the c/t pathway or the Z/E pathway. By projecting these IRC vectors upon the planes spanned by GD and NADC, we can obtain information on the local orientation of the IRC relative to the branching space. The value of the angle between the IRC vectors and this plane is about 75.0° at both optimized conical intersection points. This is pictorially illustrated in Figure 9. Thus the direction of the excited-state trajectory (and of its corresponding momentum) does not lie in the branching space defined by the vectors $\mathbf{x}_1$ and $\mathbf{x}_2$. This feature may cause large changes in the original direction of the motion during the decay. However, as we shall discuss in more detail subsequently, we can expect that some of the ground-state trajectories leading to a final photoproduct will simply originate from the IRC that begins on the excited state.

4. Comparison with Experimental Results

We believe that we have demonstrated that the potential surface of the 2^1A_g state of *cis*-hexatriene contains two low-lying conical intersection points that are connected to an excited-state reactant via two distinct excited-state reaction pathways involving cis–trans isomerization motion. The structures, and energies of the two transition states located along these pathways dictate that the optimized conical intersection points are the "products" of the excited-state "reaction" and that they are readily accessible

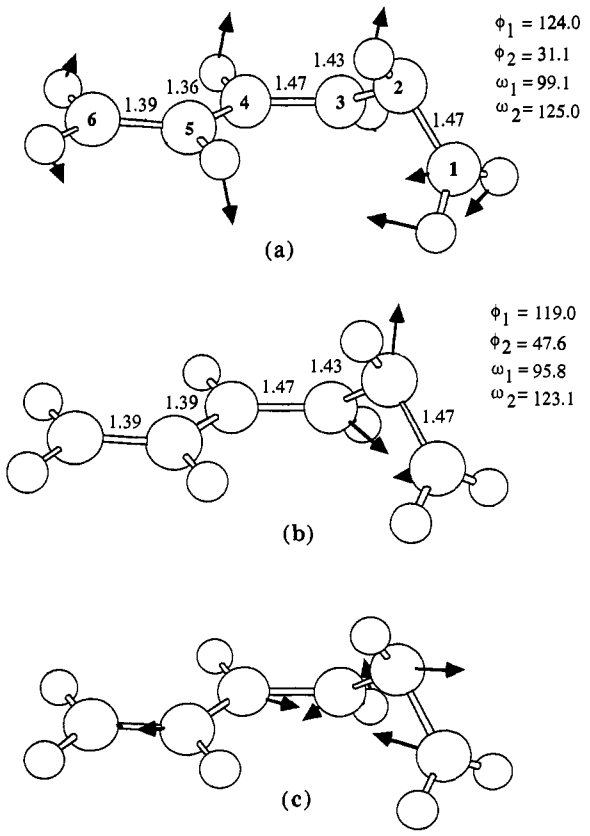

Figure 7. (a) Structure of the last c/t IRC point (point V in Figures 5a and 6a). The arrows indicate the direction of the main atomic displacements corresponding to the IRC vector. (b) Optimized CAS-SCF/4-31G c/t conical intersection structure. The arrows indicate the direction of the main atomic displacements corresponding to the NADC vector. (c) Same as a, but the arrows indicate the direction of the main atomic displacements corresponding to the GD vector. The values of the more relevant bond lengths and bond angles (defined in Scheme 2) are in angstroms and degrees.

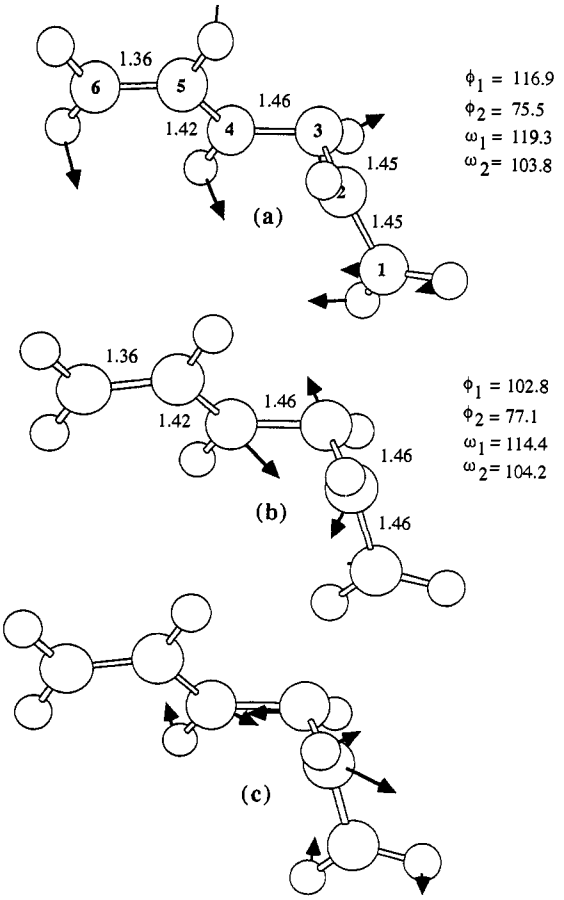

Figure 8. (a) Structure of the last Z/E IRC point (point V in Figures 5b and 6b). The arrows indicate the direction of the main atomic displacements corresponding to the IRC vector. (b) Optimized CAS-SCF/4-31G Z/E conical intersection structure. The arrows indicate the direction of the main atomic displacements corresponding to the NADC vector. (c) Same as a, but the arrows indicate the direction of the main atomic displacements corresponding to the GD vector. The values of the more relevant bond lengths and bond angles (defined in Scheme 2) are in angstroms and degrees.

by overcoming a small barrier. Thus, the *complete* reaction pathway for the cis–trans photoisomerization of *tZt*-hexatriene must involve two stages. During the first stage, the excited-state reactant[15] follows the c/t or Z/E isomerization path described above and enters the Born–Oppenheimer violation region surrounding the conical intersection point where decay from the excited state to the ground state takes place. After the decay, the reaction enters the second stage, where the system relaxes on the ground-state potential energy surface following one or more pathways leading up to the final products of the photoreaction.

The actual prediction of relative or absolute product quantum yields for a photochemical reaction occurring via the mechanism discussed above requires a dynamical description of both the adiabatic motion on the excited- and ground-state sheets and nonadiabatic processes describing the radiationless decay from the upper to the lower surface. This decay would involve the entire Born–Oppenheimer violation region surrounding any effective (i.e., accessible) conical intersection point. While different methods have been proposed for carrying out this type of study (see, for example, ref 16), a quantitative treatment of the dynamics of the reaction under investigation is not yet possible for a system of this size. Nevertheless, the data presented in the previous section provide a certain amount of qualitative information on the nature of the photoproducts that result from the irradiation of *cis*-hexatriene. We now give some discussion of this point.

In order to rationalize the experimental data available on *cis*-hexatriene photochemistry, one needs to describe, at least qualitatively, the nature of the second stage of the mechanism: the ground-state relaxation pathways. Both the geometric structure and the wave function corresponding to the conical intersection points $CI_{c/t}$ and $CI_{Z/E}$ support the idea that at the moment of the decay the system is basically a tetraradical. In particular, the two structures have three quasilocalized electrons on carbons 1, 2, and 3 and a fourth electron delocalized on the allyl-like fragment formed by carbons 4, 5, and 6 (in the case of $CI_{Z/E}$, the fourth electron seems almost localized on carbon 4 as indicated in Scheme 4. The tetraradicaloid electronic structure of the system implies that after the decay the system will be very unstable due to the lack of bonding. Thus, the subsequent relaxation onto the ground-state sheet will be dominated by concerted or stepwise bond-making processes that correspond to recoupling of the four quasiunpaired electrons. In Scheme 4, we have reported a schematic representation of some of the possible bond-making/electron-recoupling processes which might occur along different ground-state relaxation paths.

The fact that both the c/t and Z/E reaction pathways enter the Born–Oppenheimer violation region at less than one-third of the way along the pathway for cis–trans isomerization supports the conjecture that the majority of excited-state molecules will

(15) Radiationless decay from the spectroscopically allowed 1^1B_u to the forbidden (first excited) 2^1A_g state seems to occur without any significant geometrical distortion in butadienes (see, for example, Trulson, M. O.; Mathies, R. A. *J. Chem. Phys.* **1990**, *94*, 5741–5747). We assume a similar behavior for hexa-1,3,5-trienes (see also ref 5b).

(16) Herman, M. F. *J. Chem. Phys.* **1984**, *81*, 754–763.

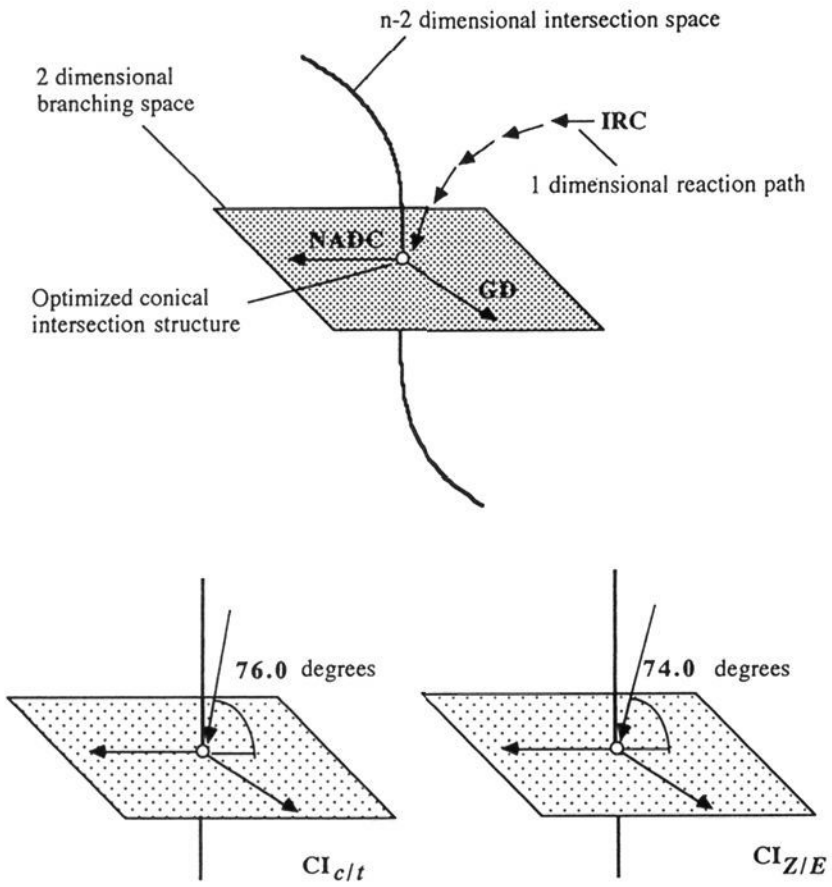

Figure 9. Schematic illustration of the "spatial relationship" between the intersection space, branching space, and IRC in the vicinity of the two optimized conical intersection points. The local values of the angles between the branching space and the IRC vector computed on point V (see Figures 7 and 8) are reported in degrees for both the $CI_{c/t}$ and the $CI_{Z/E}$ points.

Scheme 4

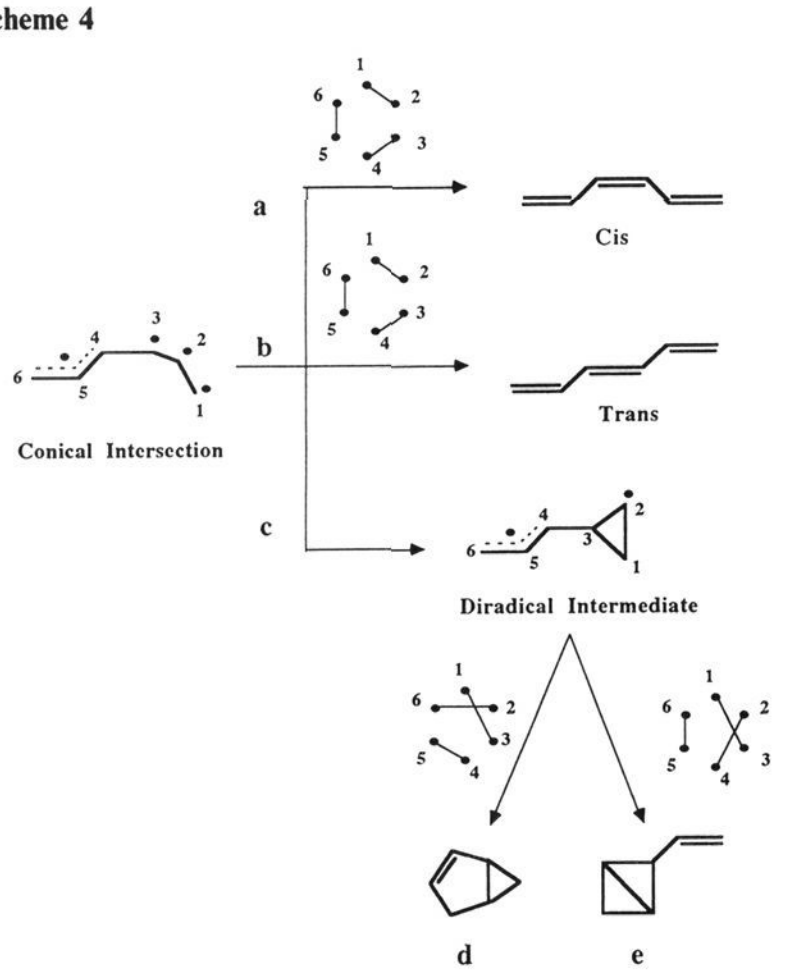

decay back to the ground-state reactant (see path a in Scheme 4). This behavior is also consistent with the nature of the NADC and GD vectors displayed in Figures 7 and 8 since, as already discussed in the previous section, the main fraction of the initial decay trajectories from the conical intersection will have a large component on the plane spanned by these two vectors. In fact, GD is dominated by the stretching modes associated with double-bond back-formation, while NADC is associated with modes leading back toward planar structures. Thus, we can expect a low absolute quantum yield for cis–trans isomerization of *cis*-hexatriene. A second cause of the low quantum yield associated with cis–trans isomerization could be related to the fact that the two excited-state isomerization pathways are competitive. In particular, the magnitudes of the barriers shown in Table 1 are consistent with a c/t process that is faster than the Z/E process. This fact should contribute to decrease the quantum yield for cis–trans isomerization since the product of a c/t isomerization is just a different conformer and not a new cis–trans isomer of the starting reactant.

Experimental data from both solution photochemistry and matrix isolation experiments reveal low efficiency in the photoproduction of *trans*-hexatriene from *cis*-hexatriene. Havinga and Jacobs reported[1a,c] that irradiation of a 1% pentane solution of *cis*-hexatriene carried out at room temperature using a 265-nm wavelength led to cis–trans isomerization with a 0.034 quantum yield only. A matrix isolation study of the photochemical transformation of *cis*-hexatriene has been instead published by Boikess *et al.*,[17] where the experimental conditions (20 K in argon matrix) ensured an almost negligible vibrational excess energy during the photoreaction. The authors reported that only a small fraction of *cis*-hexatriene was transformed in *trans*-hexatriene after 8 h of irradiation.

The small fraction of the excited-state molecules that do actually produce *trans*-hexatriene (path b in Scheme 4), presumably by following the Z/E isomerization pathway, undergo a bond-making/electron-recoupling process that is identical to the one which leads back to the reactant. However, rather than following an initial trajectory lying mainly on the branching space, the IRC path is continued on the ground state. As we have indicated previously, the excited-state IRC path does not lie in the plane x_1x_2. Since the geometry of the $CI_{Z/E}$ has both π bonds broken, the energy of $CI_{Z/E}$ lies above any ground-state cis-trans isomerization transition state where only one double bond is broken and a 90° twisted diallyl diradical structure is assumed (see, for example, ref 18). Thus, the isomerization can occur by simply continuing on the ground state the pathway begun on the excited state. However, in solution, the system will loose energy very rapidly to the condensed medium, and the probability of forming *trans*-hexatriene and other products will be low.

The kind of behavior described above can explain not only the photochemical production of *trans*-hexatriene but also the simultaneous production of other even less important, but detectable, photoproducts of *cis*-hexatriene. The first of these products seems to be formed simultaneously with *trans*-hexatriene during irradiation of matrix-isolated *cis*-hexatriene, as reported by Boikess *et al.*[17] These authors detected by infrared spectroscopy a thermally unstable photoproduct which accumulated in the matrix at 20 K. This product has been tentatively identified as 2-vinylbicyclo[1.1.0]butane. Our IRC computation indicates that the formation of that product can indeed arise during irradiation of *cis*-butadiene via the c/t isomerization pathway. After the $TS_{c/t}$ transition structure, the IRC acquires a large component in the ω_1 variable describing the closure of the bending angle formed by the carbon atoms 1, 2, and 3. Thus, the momentum directed along the c/t IRC describes not only a c/t isomerization process but also a more sterically demanding simultaneous three-member ring formation via coupling of the electrons on carbons 1 and 3. The process leads to formation of a ground-state 1,3-diradical intermediate (see path c in Scheme 4), which in turn can undergo either a ring-opening back to the reactant or a further ring-closure process. In this last case, the reaction leads to two different bicyclic products. The 2-vinylbicyclo[1.1.0]butane (see structure e in Scheme 4) is thermally unstable and disappears when the sample obtained in the matrix isolation experiment is warmed up to room temperature. A second possible bicyclic

(17) Datta, P.; Goldfarb, T. D.; Boikess, R. S. *J. Am. Chem. Soc.* **1971**, *93*, 5189–5193.
(18) Doering, W. von E.; Kitagawa, T. *J. Am. Chem. Soc.* **1991**, *113*, 4288–4297.
(19) Spitznagel, G. W.; Clark, T.; Chandrasekhar, J.; Schleyer, P. v. R. *J. Comput. Chem.* **1982**, *3*, 363–371.

product, i.e., bicyclo[3.1.0]hexene (structure d in Scheme 4), would be more difficult to form via electron-recoupling because of the larger distance between the centers holding the two unpaired electrons (i.e., carbons 2 and 6). However, this compound is thermally stable and should accumulate, over long irradiation times, in the reaction mixture. Bicyclo[3.1.0]hexene is in fact observed[1a] in a significant amount after a long irradiation time at room temperature (about 6 times the time necessary for cis–trans hexatriene photoequilibration), as expected for a very low quantum yield irreversible transformation.

While the existence of the two low-lying accessible conical intersection points $CI_{c/t}$ and $CI_{Z/E}$ can explain the observed photochemical behavior, the question remains whether the two conical intersections found on the 2^1A_g state correspond to the main radiationless decay channels observed in photophysics experiments. Christensen, Yoshihara, *et al.*[5a] have observed, for the first time, the fluorescence excitation spectra of isolated *cis*-hexatriene in a cool jet. Analysis of their data reveals the existence of two different radiationless decay channels which are accessible by overcoming different barriers. The first channel is basically barrierless and causes the fluorescence quantum yield to be significantly less than 1.00 even at the origin of the spectra. The second radiationless decay channel opens up by overcoming a barrier of less than 1 kcal mol^{-1}. Our computed barriers to the two conical intersection points are larger than the observed ones. A CAS-SCF/DZ+d calculation is certainly adequate for mechanistic investigation (i.e., the surface topology is correct). Thus we can have a high level of confidence that the conical intersections do indeed form the observed decay channels. However, the quantitative prediction of barrier heights requires the computation of the dynamic correlation effect which is not included at this computational level.

5. Conclusions

The results presented above support the hypothesis that the photochemical cis–trans isomerization in *cis*-hexatrienes is a nonadiabatic process. As shown in Figures 5 and 6, there are two distinct cis–trans isomerization pathways which begin at the excited-state (2^1A_g) reactant well and terminate (after passing over small barriers) in two different Born–Oppenheimer violation regions where fully efficient decay to the ground-state potential energy surface is possible. The evolution of the excited-state reactant along these two reaction pathways (see Figures 3 and 4) is characterized by simultaneous torsion of the hexatriene carbon framework and of one terminal CH_2 group. In the Born–Oppenheimer violation region, the electronic structure is essentially that of a tetraradicaloid. The four quasi-unpaired electrons, after decay to the ground state, must recouple in several different ways in a bond-forming process leading to different photoproducts or back to the original reactant. The actual decay process is predicted to take place at about one-third of the way along the idealized (i.e., 180° rotation) cis–trans isomerization pathways where two structurally different conical intersection points have been located. Since it is known that in the region surrounding a conical intersection point there is a high probability of radiationless decay to the ground state, the two structures $CI_{c/t}$ and $CI_{Z/E}$ may be seen as photochemical analogs of "thermal" transition structures.

The photophysics and photochemistry of *cis*-hexatriene appear to have a common origin associated with the existence and accessibility of low-lying conical intersections on the 2^1A_g potential energy surface. Although the magnitude of the excited-state barriers to the conical intersection regions computed at the CAS-SCF/DZ+d level of theory for *cis*-hexatriene are larger than the corresponding values observed by Christensen, Yoshihara, Bell, and Petek,[5a] there can be little doubt that the two observed radiationless decay channels actually correspond to the two conical intersection points, located along the cis–trans isomerization pathways described in this article. The results presented here, together with our previous work on the photochemistry of butadiene,[4] appear to give convincing evidence that low-lying conical intersections are a common feature in short polyenes and that they are directly involved in polyene photochemistry and photophysics.

Acknowledgment. This research has been supported (in part) by the SERC (U.K.) under Grant Number GR/G 03335. The authors are also grateful to IBM for support under a Joint Study Agreement. All computations were run on an IBM RS6000.